Electronic supplementary information for

Water-enabled crystallization of mesoporous SnO_2 as binder-free electrode of enhanced sodium storage

Haidong Bian[a,b], Ranran Dong[c], Qinguo Shao[a,b], Shuo Wang[a], Muk-Fung Yuen[a,c], Zhengyu Zhang[a,c], Denis Y.W.Yu[a], Wenjun Zhang[a,c], Jian Lu[b,d,]*, Yang Yang Li[a,c,e,]*

---

[a] Center of Super-Diamond and Advanced Films (COSDAF), City University of Hong Kong, Kowloon, Hong Kong, China.

[b] Department of Mechanical and Biomedical Engineering, City University of Hong Kong, Kowloon, Hong Kong, China.

[c] Department of Physics and Materials Science, City University of Hong Kong, Kowloon, Hong Kong, China.

[d] Centre for Advanced Structural Materials, City University of Hong Kong Shenzhen Research Institute, 8 Yuexing 1st Road, Shenzhen Hi-Tech Industrial Park, Nanshan District, Shenzhen, China

[e] City University of Hong Kong Shenzhen Research Institute, 8 Yuexing 1st Road, Shenzhen Hi-Tech Industrial Park, Nanshan District, Shenzhen, China

*E-mail: jianlu@cityu.edu.hk; yangli@cityu.edu.hk

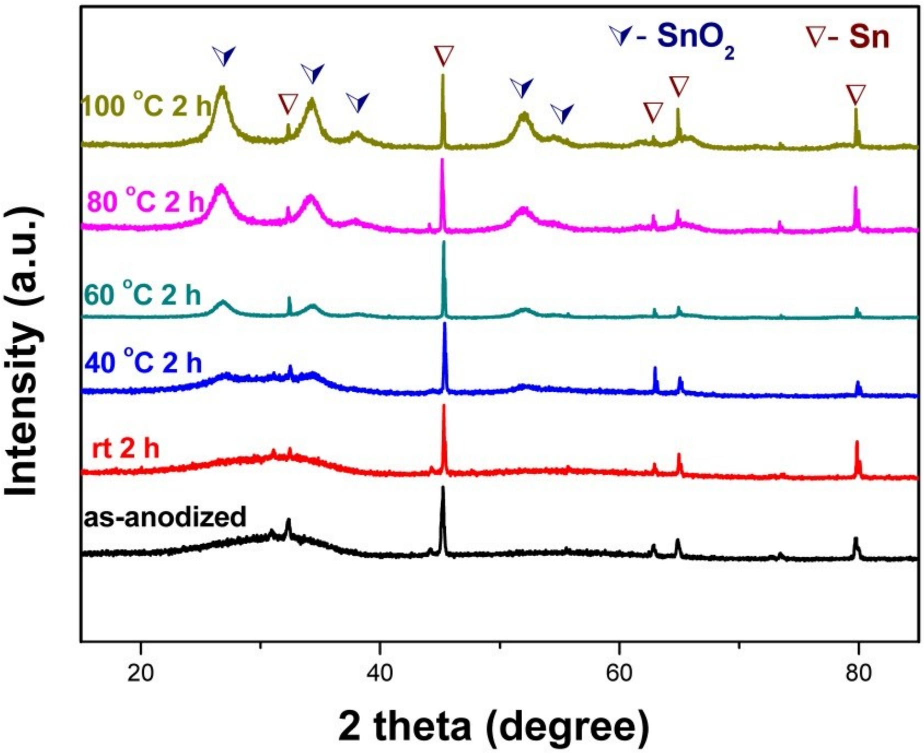

Figure S1. XRD patterns of the as-anodized SnO$_2$ film before and after water-soaking for 2 hrs at different temperature (rt, 40 ^{o}C, 60 ^{o}C, 80 ^{o}C and 100 ^{o}C).

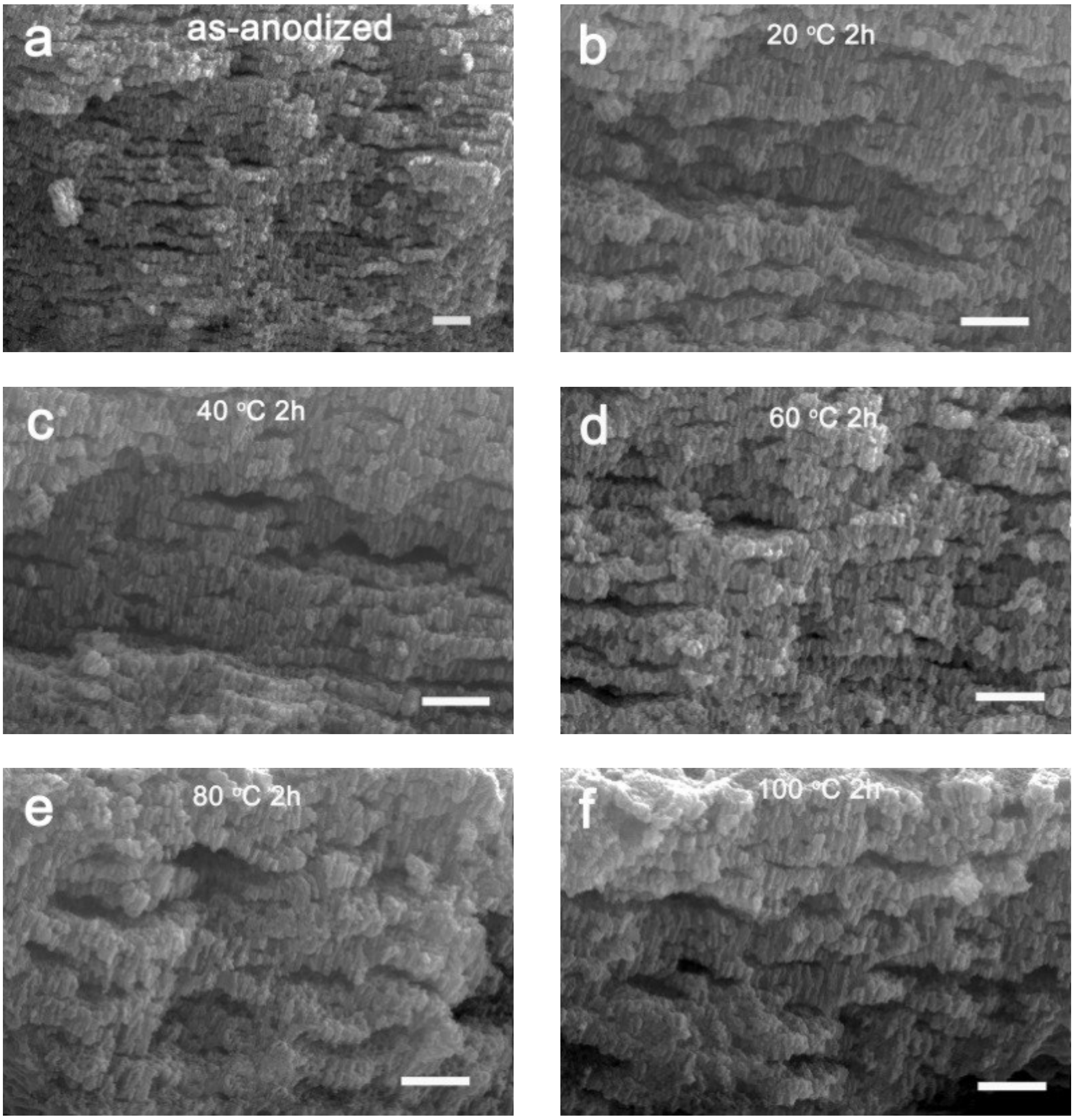

Figure S2. Cross-sectional SEM images of as-anodized SnO_2 samples before (a) and after water-soaking for 2 hrs at different temperatures (rt, 40 ^{o}C, 60 ^{o}C, 80 ^{o}C and 100 ^{o}C). Scale bars: 500 nm.

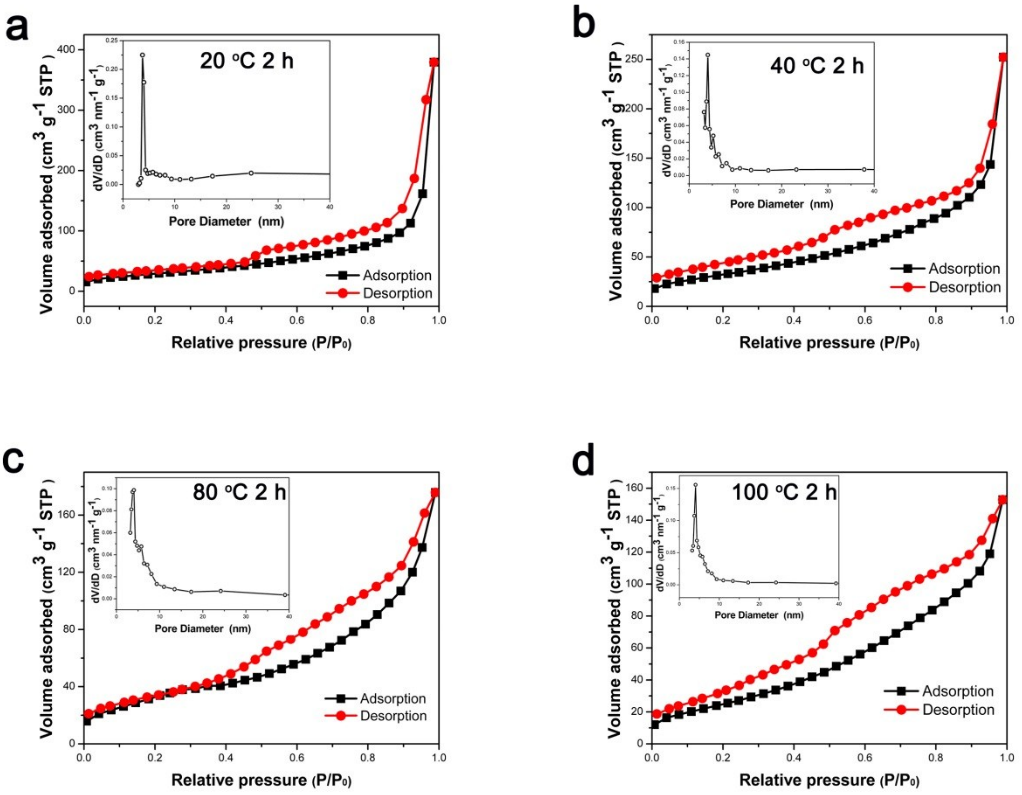

Figure S3. N_2 adsorption and desorption isotherms (measured at 77 K) of water-crystalized anodic SnO_2 at (a) 20 °C, (b) 40 °C, (c) 80 °C and (d) 100 °C. The insets are the corresponding pore-size distribution patterns calculated using the BJH method from the desorption branches.

Table S1. Surface areas and average pore sizes of the as-anodized amorphous SnO_2 and water- or thermal-crystallized SnO_2 samples, calculated from the nitrogen adsorption-desorption isotherms.

[a] Average pore size calculated using the BJH model

Treated condition	**Surface area (m^2 g^{-1})**	**Average pore size [a] (nm)**
As-anodized	98.35	3.79
20 °C for 2 hrs in water	108.18	3.76
40 °C for 2 hrs in water	122.553	4.04
60 °C for 2 hrs in water	181.45	3.78
80 °C for 2 hrs in water	133.783	4.34
100 °C for 2 hrs in water	110.918	4.07
400 °C for 2hrs in Ar	54.55	3.89

Table S2. Recent studies on SnO_2-based materials for NIBs.

Structure	**Reversible capacity (mA h/g)**	**Cycles**	**Voltage (vs.Na^+/Na)**	**Current rate**	**W/ binder?**	**Fabrication method**	**Ref.**
Mesoporous SnO_2	**514**	**100**	**0.01-2.0**	**0.1 C**	**N**	**anodization method**	**This work**
a-SnO_2/GA	380.2	100	0.01-3.0	50 mA/g	Y	hydrothermal method	[1]
SnO_2 @MWCNT nanocomposite	< 400	50	0.01-2.0	0.1 C	Y	solvothermal method	[2]
SnO_2 nanoparticle loading onto RGO	330	150	0.005 – 2.5	0.2 C	Y	Solution based percipitation	[3]
SnO_2 nanoparticles @ 3D-graphene	432	200	0.01-2.5	100 mA/g	Y	hydrothermal assembly with ice-templated 3-DG	[4]
SnO_2 / graphene	283	100	0.01-3.0	20 mA/g	Y	hydrothermal method	[5]
SnO_2 / Carbon	270	200	0.01-1.5	80 mA/g	Y	hydrothermal method	[6]
1-D nanoporous SnO_2	326	200	0.005-2.0	0.2 C	N	anodization method	[7]
SnO_2 / graphene nanocomposite	302	100	0-3.0	160 mA/g	Y	hydrothermal method	[8]
Octahedral SnO_2 nanocrystals	< 200	100	0.01-3.0	160 mA/g	Y	hydrothermal method	[9]
SnO_2 @ graphene nanocomposite	270	100	0.1-2.5	100 mA/g	Y	wet mechano-chemical process	[10]
Mesoporous SnO_x nanosheets	404	100	0.01-2.0	100 mA/g	N	anodization method	[11]

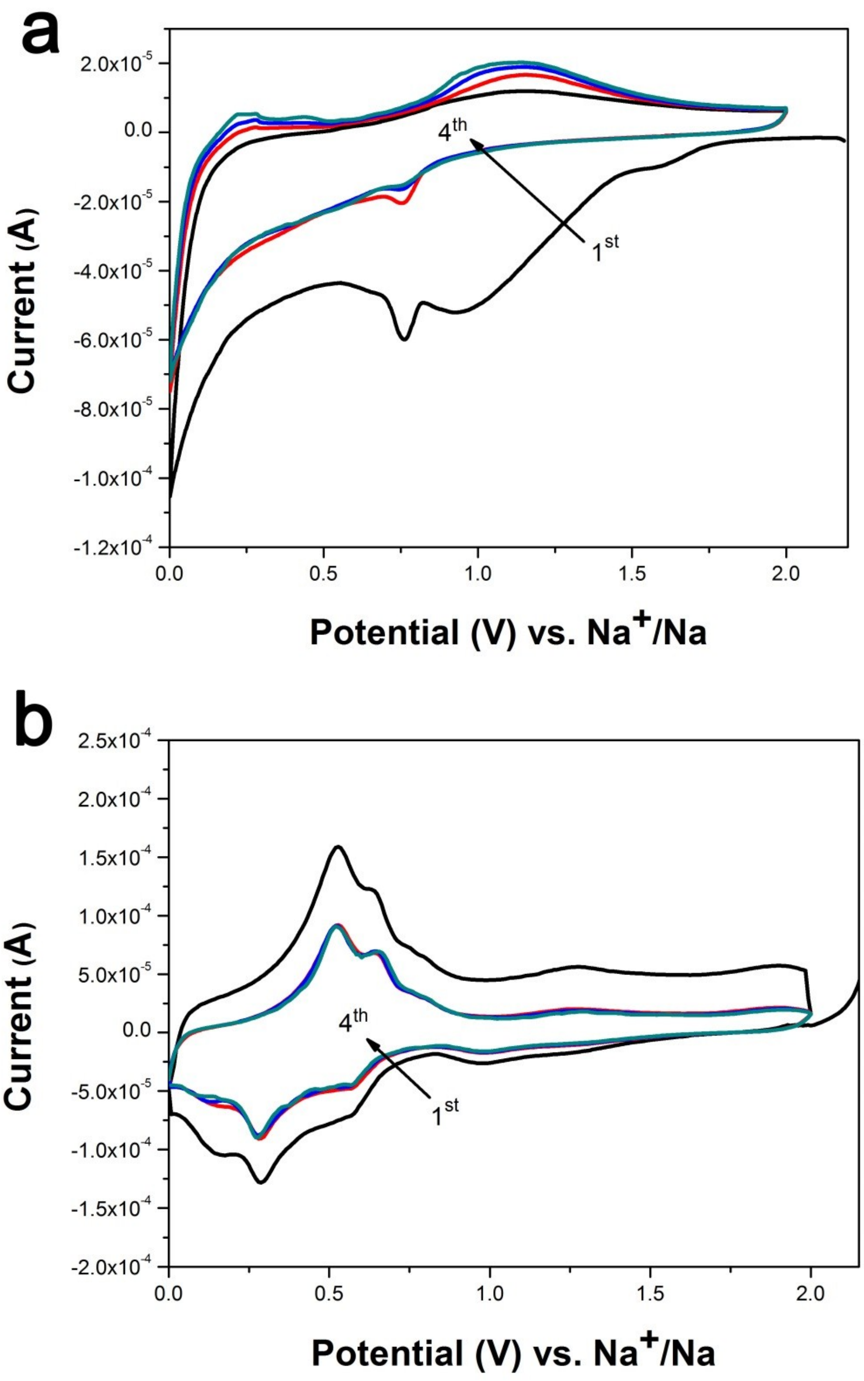

Figure S4. Cyclic voltammetry curves of a) as-anodized and b) thermally-crystallized (400 °C for 2 hrs) SnO_2 electrodes at 0.1 mV s^{-1} between 0 and 2.0 V *vs.* Na^+/Na.

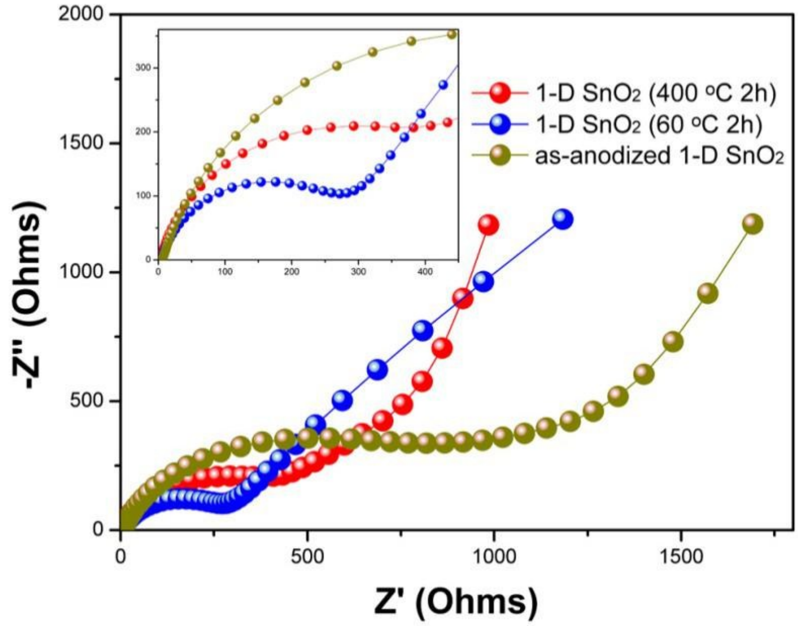

Figure S5. Nyquist plots of the as-anodized SnO_2, water-crystallized SnO_2 (60 ^{o}C for 2 hrs) and thermal-crystallized SnO_2 (400 ^{o}C for 2 hrs), measured at an amplitude of 5 mV over a frequency range from 100 kHz to 0.01 Hz.

Reference

1 L. Fan, X. Li, B. Yan, J. Feng, D. Xiong, D. Li, L. Gu, Y. Wen, S. Lawes and X. Sun, *Adv. Energy Mater.*, 2016, **6**, 1502057.

2 Y. Wang, D. Su, C. Wang and G. Wang, *Electrochem. Commun.*, 2013, **29**, 8-11.

3 Y.-X. Wang, Y.-G. Lim, M.-S. Park, S.-L. Chou, J. H. Kim, H.-K. Liu, S.-X. Dou and Y.-J. Kim, *J. Mater. Chem. A*, 2014, **2**, 529-534.

4 L. Pei, Q. Jin, Z. Zhu, Q. Zhao, J. Liang and J. Chen, *Nano Res.*, 2015, **8**, 184-192.

5 X. Xie, D. Su, J. Zhang, S. Chen, A. K. Mondal and G. Wang, *Nanoscale*, 2015, **7**, 3164-3172.

6 J. Ding, Z. Li, H. Wang, K. Cui, A. Kohandehghan, X. Tan, D. Karpuzov and D. Mitlin, *J. Mater. Chem. A*, 2015, **3**, 7100-7111.

7 H. Bian, J. Zhang, M.-F. Yuen, W. Kang, Y. Zhan, D. Y. W. Yu, Z. Xu and Y. Y. Li, *J. Power Sources*, 2016, **307**, 634-640.

8 D. Su, H.-J. Ahn and G. Wang, *Chem. Commun.*, 2013, **49**, 3131-3133.

9 D. Su, C. Wang, H. Ahn and G. Wang, *PCCP*, 2013, **15**, 12543-12550.

10 S. Li, Y. Wang, J. Qiu, M. Ling, H. Wang, W. Martens and S. Zhang, *RSC Adv.*, 2014, **4**, 50148-50152.

11 H. Bian, X. Xiao, S. Zeng, M.-F. Yuen, Z. Li, W. Kang, D. Y. W. Yu, Z. Xu, J. Lu and Y. Y. Li, *J. Mater. Chem. A*, 2017, **5**, 2243-2250.